LUND UNIVERSITY

Transient wave propagation in composite media: A Green functions approach

Karlsson, Anders; Otterheim, Henrik; Stewart, Rodney

1992

[Link to publication](#)

Transient wave propagation in composite media: A Green functions approach

Anders Karlsson, Henrik Otterheim, and Rodney Stewart

Department of Electroscience
Electromagnetic Theory
Lund Institute of Technology
Sweden

Anders Karlsson

Department of Electromagnetic Theory
Lund Institute of Technology
P.O. Box 118
SE-221 00 Lund
Sweden

Henrik Otterheim
Rodney Stewart

Department of Electromagnetic Theory
Royal Institute of Technology
SE-100 44 Stockholm
Sweden

Abstract

A generalized Green functions technique for wave propagation of transient fields in one-dimensional media is developed. The medium is partitioned into an arbitrary number of subslabs for which Green operators, that map the incident field to the internal fields, are defined. Relations between the Green operators for the entire medium and the Green operators for the subslabs are derived. The technique leads to fast numerical algorithms which are especially efficient for dispersive media. The numerical examples focus on the comparison between wave propagation in dispersive and non-dispersive media.

1 Introduction

Wave propagation of transient waves in one-dimensional inhomogeneous media is an area where time-domain techniques are often superior to frequency domain techniques. In a recent paper [1] a new solution technique in the time domain, called the Green function technique, was developed for wave propagation in non-dispersive inhomogeneous media. In this method Green operators are introduced that map an incident field to the internal fields. The Green operators are represented by kernels that satisfy hyperbolic equations. The hyperbolic equations are suitable for numerical treatment and can be used for the solution of the direct scattering problem as well as the inverse scattering problem. The technique has been applied to different types of dispersive media for both direct and inverse scattering problems, cf. [2]- [4]. The Green functions technique is related to the invariant imbedding technique which also has been applied to several direct and inverse scattering problems, cf [5], [6] and [7]- [9]. Both methods are based upon a wave splitting technique. A review of other time domain methods that are related to the Green functions technique and the invariant imbedding method can be found in [10].

In the present paper the Green functions technique is generalized to a one-dimensional medium partitioned into an arbitrary number of inhomogeneous subslabs. In this new technique, Green operators for the subslabs are introduced and relations between the Green operators for the whole medium and the Green operators for the subslabs are derived. This technique leads to algorithms suitable for parallel processing. Two different relations are found, whose basic difference lies in the choice of boundary conditions used for the subslabs. The first relation is obtained by a technique analogous to the imbedding technique, cf [5]. The second relation uses the Redheffer star product, cf [11] and [9]. The new technique can be applied to wave propagation in any one-dimensional linear medium, but only dispersive inhomogeneous media will be considered in this paper. Computationally the original Green functions technique is very memory requiring for wave propagation problems for dispersive media, so that the class of dispersive problems that this technique can be applied to is limited. In the partitioning technique developed in this paper the memory requirements are considerably smaller and therefore a much larger class of wave propagation problems for dispersive media can be handled numerically. In the numerical examples the new technique is applied to dispersive wave propagation problems for which the original technique is too memory requiring.

The outline of the paper is as follows. In section 2 the wave equation is derived for dispersive media and the wave splitting is defined. In section 3 the Green operators and kernels for the entire medium are introduced and the equations for the Green kernels are derived. The corresponding equations for the non-dispersive case will not be presented, cf [1]. In section 4 the scattering medium is partitioned in subslabs and the corresponding Green operators for these imbedded slabs are introduced. The connection between the Green operators for the imbedded slabs and the Green operator for the whole medium is also given in this section. The numerical section contains a presentation of the most common models for dispersive media and numerical examples of wave propagation in these media. The new technique makes it possible to study wave propagation in these dispersive media as their properties approach those of non-dispersive dielectric media. Numerically these wave propagation problems require high accuracy and serve as good tests for the numerical algorithms.

2 The wave equation and wave splitting

The solution technique described in the two following sections is general and may be applied to any linear one-dimensional medium. For the sake of clarity the method will only be exemplified explicitly for a dispersive medium. The constitutive relations, the wave equation and the corresponding wave splitting for a dispersive medium will be given in this section.

Linear isotropic dispersive media can mostly be described by the electric susceptibility kernel, χ_e, and the magnetic susceptibility kernel, χ_m, in the following manner

$$\boldsymbol{D}(\boldsymbol{r}, t) = \varepsilon_0(\boldsymbol{E}(\boldsymbol{r}, t) + \int_{-\infty}^{t} \chi_e(\boldsymbol{r}, t - t')\boldsymbol{E}(\boldsymbol{r}, t') \, dt'), \qquad (2.1)$$

$$\boldsymbol{B}(\boldsymbol{r}, t) = \mu_0(\boldsymbol{H}(\boldsymbol{r}, t) + \int_{-\infty}^{t} \chi_m(\boldsymbol{r}, t - t')\boldsymbol{H}(\boldsymbol{r}, t') \, dt'). \qquad (2.2)$$

The constitutive relations in the time domain follow from arguments based upon invariance under time translation and causality, cf Ref. [12]. There are more general constitutive relations if the media are chiral or biisotropic, cf Ref. [12], but these are not to be addressed in this paper. In the paper only non-magnetic materials will be considered and thus $\chi_m(\boldsymbol{r}, t) = 0$. From now on the electric susceptibility kernels will simply be called susceptibility kernels and will be denoted as χ. A discussion of two specific models for the susceptibility kernel is given in the numerical section.

The medium varies with depth z only and the incident wave is planar and normally incident. Without lack of generality the electric field can be considered to have only one component, denoted $E(z, t)$. It is assumed that the electric field in the medium is zero prior to $t = 0$. The wave equation for the electric field for a dispersive medium is obtained from the Maxwell equations and the relation in Eq.

(2.1), it reads

$$\partial_z^2 E(z,t) - \frac{1}{c_0^2}\left\{\partial_t^2 E(z,t) + [\chi * \partial_t^2 E](z,t)\right\} = 0, \tag{2.3}$$

where $c_0 = (\mu_0\varepsilon_0)^{-1/2}$ is the speed of light in vacuum. The following notation for convolution integral has been introduced:

$$[f * g](z,t) = \int_0^t f(z,t-t')g(z,t')\,dt'. \tag{2.4}$$

The wave equation, rewritten as a system of first order PDE:s, then reads

$$\partial_z \begin{pmatrix} E \\ \partial_z E \end{pmatrix} = \begin{pmatrix} 0 & 1 \\ \frac{1}{c_0^2}\{\partial_t^2 + [\chi * \partial_t^2]\} & 0 \end{pmatrix} \begin{pmatrix} E \\ \partial_z E \end{pmatrix} = \mathbf{A}\begin{pmatrix} E \\ \partial_z E \end{pmatrix}. \tag{2.5}$$

The wave splitting is now done according to the principal part, $\partial_z^2 - c_0^{-2}\partial_t^2$, of the wave equation. Thus the following change of basis is introduced:

$$E^{\pm}(z,t) = \frac{1}{2}\left\{E(z,t) \mp c_0\int_0^t \partial_z E(z,t')\,dt'\right\}. \tag{2.6}$$

In vacuum, the split fields $E^{\pm}$ correspond to left (negative z direction) and right (positive z direction) moving waves. In a matrix form the change of basis reads

$$\begin{pmatrix} E^+ \\ E^- \end{pmatrix} = \frac{1}{2}\begin{pmatrix} 1 & -c_0\partial_t^{-1} \\ 1 & c_0\partial_t^{-1} \end{pmatrix}\begin{pmatrix} E \\ \partial_z E \end{pmatrix} = \mathbf{P}\begin{pmatrix} E \\ \partial_z E \end{pmatrix} \tag{2.7}$$

where ∂_t^{-1} denotes integration in time. Thus the split fields E^+ and E^- satisfy the following relations

$$\begin{cases} E^+ + E^- = E \\ E^- - E^+ = c_0\partial_t^{-1}\partial_z E. \end{cases} \tag{2.8}$$

The inverse of the matrix operator $\mathbf{P}$ reads

$$\mathbf{P}^{-1} = \begin{pmatrix} 1 & 1 \\ -c_0^{-1}\partial_t & c_0^{-1}\partial_t \end{pmatrix}. \tag{2.9}$$

The wave equation may now be written in terms of the new basis $E^{\pm}$ as

$$\partial_z \begin{pmatrix} E^+ \\ E^- \end{pmatrix} = \mathbf{P}\mathbf{A}\mathbf{P}^{-1}\begin{pmatrix} E^+ \\ E^- \end{pmatrix} = \begin{pmatrix} \alpha & \beta \\ -\beta & -\alpha \end{pmatrix}\begin{pmatrix} E^+ \\ E^- \end{pmatrix} \tag{2.10}$$

where

$$\begin{cases} \alpha = -\dfrac{1}{c_0}\partial_t - \dfrac{1}{2c_0}\chi * \partial_t \\[2mm] \beta = -\dfrac{1}{2c_0}\chi * \partial_t \end{cases} \tag{2.11}$$

3 The Green functions method

In this section the Green operators, that map the incident field to the internal fields, are introduced and the corresponding PDE:s for the Green kernels are derived. Similar presentations are found in, e.g. [1], [4] and [3]. The advantage of introducing Green operators is that they are fundamental solutions to the wave equation, independent of the incident field and are thus given solely by the medium.

Consider a slab extending from $z = 0$ to $z = L$ of dispersive media. Outside the slab there is vacuum. For a wave propagating in the positive $z-$direction and incident at $z = 0$ the following relations may be verified by arguments based upon invariance under time translation and causality:

$$\begin{pmatrix} E^+ \\ E^- \end{pmatrix}(z, t + z/c_0) = \begin{pmatrix} \mathcal{G}^+(z) \\ \mathcal{G}^-(z) \end{pmatrix} E^+(0, t) = \tag{3.1}$$

$$= \begin{pmatrix} a(0, z) \\ 0 \end{pmatrix} E^+(0, t) + \left[\begin{pmatrix} G^+(z, \cdot) \\ G^-(z, \cdot) \end{pmatrix} * E^+(0, \cdot) \right](t),$$

where

$$a(z_0, z_1) = \exp\left(-\int_{z_0}^{z_1} \chi(z', 0)\, dz'/2c_0 \right). \tag{3.2}$$

is the attenuation of the wave front. The operators $\mathcal{G}^+(z)$ and $\mathcal{G}^-(z)$ are called the Green operators and the kernels $G^\pm(z, t)$ are referred to as the Green kernels. The time dependence in the operators is suppressed in the argument.

One also may introduce Green operators $\mathcal{F}^\pm$ and Green kernels $F^\pm(z, t)$ for a wave propagating in the negative $z-$direction and incident at $z = L$. Thus

$$\begin{pmatrix} E^+ \\ E^- \end{pmatrix}(z, t + (L - z)/c_0) = \begin{pmatrix} \mathcal{F}^+ \\ \mathcal{F}^- \end{pmatrix} E^-(L, t) = \tag{3.3}$$

$$= \begin{pmatrix} 0 \\ a(z, L) \end{pmatrix} E^-(L, t) + \left[\begin{pmatrix} F^+(z, \cdot) \\ F^-(z, \cdot) \end{pmatrix} * E^-(L, \cdot) \right](t).$$

In the representations in Eqs. (3.1) and (3.3) wave front time is used. This means that $t = 0$ at a point z when the wave front passes that point. Thus time is shifted an amount $\tau = z/c_0$ and $\tau = (L - z)/c_0$, respectively, compared to an absolute time where time is zero when the incident wave hits the respective surface of the slab.

The equations for the kernels $G^\pm$ are now derived. The derivation of the corresponding equations for the kernels $F^\pm$ is analogous. Differentiation of Eq. (3.1) with respect to z gives

$$\left(\partial_z + \frac{1}{c_0} \partial_t \right) \begin{pmatrix} E^+ \\ E^- \end{pmatrix}(z, t + \frac{z}{c_0}) = \begin{pmatrix} \partial_z a(0, z) \\ 0 \end{pmatrix} E^+(0, t) +$$

$$+ \left[\begin{pmatrix} \partial_z G^+(z, \cdot) \\ \partial_z G^-(z, \cdot) \end{pmatrix} * E^+(0, \cdot) \right](t). \tag{3.4}$$

The $z-$derivative of E^+ and E^- are eliminated by the dynamics in Eq. (2.10) and thus

$$-\tfrac{1}{2c_0}\left\{\left[\partial_t\chi(z,\cdot)*(E^++E^-)(z,\cdot+\tfrac{z}{c_0})\right](t)+\chi(z,0)(E^++E^-)(z,t+\tfrac{z}{c_0})\right\}=$$
$$=\partial_z a(0,z)E^+(0,t)+\left[\partial_z G^+(z,\cdot)*E^+(0,\cdot)\right](t) \qquad (3.5)$$

$$\tfrac{1}{2c_0}\left\{\left[\partial_t\chi(z,\cdot)*(E^++E^-)(z,\cdot+\tfrac{z}{c_0})\right](t)+\chi(z,0)(E^++E^-)(z,t+\tfrac{z}{c0})\right\}+$$
$$+\tfrac{2}{c_0}\partial_t E^-(z,t+\tfrac{z}{c_0})=\left[\partial_z G^-(z,\cdot)*E^+(0,\cdot)\right](t) \qquad (3.6)$$

By using the representation in Eq. (3.1) it is seen that E^- can be eliminated giving

$$-\frac{1}{2c_0}\left\{a(0,z)[\partial_t\chi*E^+]+[\partial_t\chi*(G^++G^-)*E^+]+\chi(z,0)a(0,z)E^++ \qquad (3.7)\right.$$
$$\left.+\chi(z,0)[(G^++G^-)*E^+]\right\}=\partial_z a(0,z)E^++[\partial_z G^+*E^+],$$

$$\frac{1}{2c_0}\left\{a(0,z)[\partial_t\chi*E^+]+[\partial_t\chi*(G^++G^-)*E^+]+\chi(z,0)a(0,z)E^++ \qquad (3.8)\right.$$
$$\left.+\chi(z,0)[(G^++G^-)*E^+]\right\}=[\partial_z G^-*E^+]-\frac{2}{c_0}([\partial_t G^-*E^+]+G^-(0)E^+)$$

where it is understood that the arguments of $E^\pm$ are $(0,t)$ and the arguments of χ and $G^\pm$ are (z,t). Identification of the terms proportional to $E^+(0,t)$ and of the terms expressed as convolutions with $E^+(0,t)$ give the following equations and initial condition:

$$\begin{cases} 2c_0\partial_z G^+(z,t)=-\partial_t\left\{a(0,z)\chi(z,t)+[\chi*(G^++G^-)](z,t)\right\} \\ \\ 2c_0\partial_z G^-(z,t)-4\partial_t G^-(z,t)=\partial_t\left\{a(0,z)\chi(z,t)+[\chi*(G^++G^-)](z,t)\right\} \end{cases} \qquad (3.9)$$

$$G^-(z,0)=-\frac{1}{4}a(0,z)\chi(z,0) \qquad (3.10)$$

$$\partial_z a(0,z)+\frac{\chi(z,0)}{2c_0}a(0,z)=0. \qquad (3.11)$$

It has then been utilized that $E^+(0,t)$ is an arbitrary incident field. From the representation in Eq. (3.1) it is seen that $a(z,z)=1$ and thus Eq. (3.11) is consistent with Eq. (3.2).

The corresponding equations and initial conditions for the kernels $F^\pm$ read

$$\begin{cases} 2c_0\partial_z F^-(z,t)=\partial_t\left\{a(z,L)\chi(z,t)+[\chi*(F^++F^-)](z,t)\right\} \\ 2c_0\partial_z F^+(z,t)+4\partial_t F^+(z,t)=-\partial_t\left\{a(z,L)\chi(z,t)+[\chi*(F^++F^-)](z,t)\right\} \end{cases}$$
$$\qquad (3.12)$$

$$F^+(z,0)=-\frac{1}{4}a(z,L)\chi(z,0). \qquad (3.13)$$

The boundary conditions of the kernels $G^{\pm}$ and $F^{\pm}$ are needed to solve the equations (3.1) and (3.3) uniquely. These boundary conditions follow from the representations in Eqs. (3.1) and (3.3) and read

$$\begin{cases} G^+(0,t) = 0 \\ G^-(L,t) = 0 \\ F^+(0,t) = 0 \\ F^-(L,t) = 0. \end{cases} \qquad (3.14)$$

It also should be noted that the boundary values $G^-(0,t)$, and $F^+(L,t)$ are the reflection kernels and $G^+(L,t)$ and $F^-(0,t)$ the transmission kernels of the medium.

4 The Green operators of a medium from Green operators of imbedded media

The objective of this section is to introduce relationships that allow one to construct the Green operators of a stratified medium from the Green operators of its imbedded media. Two different approaches are presented. In both approaches the slab is partitioned into subslabs. The approaches differ due to the different boundary conditions used for the Green kernels of the subslabs.

The first approach is referred to as the imbedded approach. Local Green kernels are then calculated for a sequence of subslabs. The local Green kernels of each subslab depends, via boundary conditions, on the local Green kernels of the previous subslab in the sequence. The approach is analogous to the imbedding method used in invariant imbedding techniques, [5].

In the other approach, the composite approach, the total medium is viewed as being a composite of independent subslabs. The local Green kernels of the subslabs are calculated assuming the subslab is imbedded in vacuum. The Green kernels of the entire medium are then constructed by combining these disjoint local Green kernels via the Redheffer star product, [11].

The disjoint approach is more complicated in its structure than the imbedded approach. The major advantage of it is that the local Green kernels are properties of the individual subslabs. Thus from a set of local Green kernels the scattering kernels of different composite media can be obtained.

Both approaches are suitable for implementation on a parallel processing computer. An algorithm based upon the imbedded approach has successfully been implemented on a N-cube machine using 128 nodes. The algorithm assigns one node of the computer for each subslab. A node only communicate with its neighbours and the only information that is transferred is the boundary conditions of the subslabs.

In the first subsection the sequential approach is discussed for the simple case of a medium partitioned in two subslabs. This subsection should be seen as an introduction to the general cases treated in the other subsections.

4.1 The imbedded approach: The simple case of two sub-slabs

In this subsection a slab is partitioned into two subslabs and the Green operators of the whole slab are obtained from the Green operators of the subslabs. The whole slab will be denoted M_0 and as in the previous section it occupies the region $0 \leq z \leq L$. In the regions $z < 0$ and $z > L$ there is vacuum. The slab is divided into two subslabs $S_0 = [0, z_1]$ and $M_1 = [z_1, L]$. Local Green operators $\mathbf{g}^{\pm}(z, M_1)$ are introduced for the subslab M_1. These operators map a field, $E^+(z_1, t)$, incident on the subslab M_1 to the internal fields of M_1. From the representation in Eq. (3.1) it follows that

$$\left(\begin{array}{c} \mathbf{g}^+(z, M_1) \\ \mathbf{g}^-(z, M_1) \end{array} \right) E^+(z_1, t) = \left(\begin{array}{c} a(z_1, z) \\ 0 \end{array} \right) E^+(z_1, t) +$$
$$+ \left[\left(\begin{array}{c} g^+(z, M_1, \cdot) \\ g^-(z, M_1, \cdot) \end{array} \right) * E^+(z_1, \cdot) \right](t), \quad z \in M_1. \qquad (4.1)$$

The initial and boundary conditions of the kernels $g^{\pm}(z, M_1, t)$ are the same as for $G^{\pm}(z, t)$ in the previous section, i.e.,

$$g^-(z, M_1, 0) = -\frac{1}{4} a(z_1, z) \chi(z, 0) \qquad (4.2)$$

$$\begin{cases} g^+(z_1, M_1, t) = 0 \\ g^-(L, M_1, t) = 0 \end{cases} \qquad (4.3)$$

Thus $\mathbf{g}^{\pm}$ are the Green operators for M_1 when M_1 is imbedded in vacuum. The kernels $g^{\pm}(z, M_1, t)$ satisfy the same equations as $G^{\pm}(z, t)$, i.e., Eq. (3.9).

A relation between the Green operators of the entire slab, $\mathcal{G}^{\pm}(z)$, and the Green operators of the subslab M_1, $\mathbf{g}^{\pm}(z, M_1)$, can be found by the following arguments. Given $E^+(0, t)$ as the input on M_0, the input on M_1 is given by $E^+(z_1, t + z_1/c_0) = \mathcal{G}^+(z_1) E^+(0, t)$. From this, the internal fields for $z \in M_1$ are given by

$$E^{\pm}(z, t + z/c_0) = \mathbf{g}^{\pm}(z, M_1) \mathcal{G}^+(z_1) E^+(0, t) \qquad (4.4)$$

and thus

$$\mathcal{G}^{\pm}(z) = \mathbf{g}^{\pm}(z, M_1) \mathcal{G}^+(z_1), \quad z \in M_1. \qquad (4.5)$$

This relation is fundamental for the partitioning techniques developed in this paper. If the material parameters are continuous across z_1, equation (4.5) can be written explicitly in terms of its kernels as

$$\begin{aligned} G^+(z, t) = \quad & a(z_1, z) G^+(z_1, t) + a(0, z_1) g^+(z, M_1, t) + \\ & + \left[g^+(z, M_1, \cdot) * G^+(z_1, \cdot) \right](t) \qquad (4.6) \\ G^-(z, t) = \quad & a(0, z_1) g^-(z, M_1, t) + \left[g^-(z, M_1, \cdot) * G^+(z_1, \cdot) \right](t), \; z \in M_1. \; (4.7) \end{aligned}$$

As a first step in an algorithm to obtain $G^{\pm}(z, t)$, the kernels $g^{\pm}(z, M_1)$ are determined from Eq. (3.9) using the boundary conditions in Eq. (4.3) and the
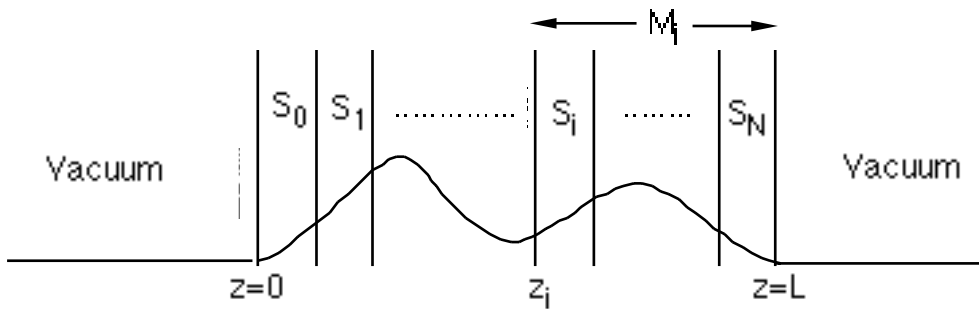
Figure 1: The partitioned medium.

initial condition in Eq. (4.2). From Eq. (4.7) it is seen that the boundary condition for $G^-(z,t)$ at $z = z_1$ reads

$$G^-(z_1, t) = a(0, z_1)g^-(z_1, M_1, t) + [g^-(z_1, M_1, \cdot) * G^+(z_1, \cdot)](t). \qquad (4.8)$$

From this boundary condition and the initial condition in Eqs. (3.10) the kernels $G^\pm(z,t)$ can be solved for the region $0 < z < z_1$ from Eq. (3.9). As a last step $G^\pm(z,t)$ has to be determined for the region $z \in M_1$. This is done from Eq. (4.5) for $z \in M_1$, since both operators on the right hand side are known at this stage.

It is straightforward to partition the slab into three subslabs. This is done by dividing the region M_1 into two regions, $S_1 = \{z : z_1 < z_2\}$ and $M_2 = \{z : z_2 < z < L\}$. The Green operators for M_1, i.e. $\mathbf{g}^\pm(z, M_1)$, will then be determined from the Green operators for M_2, i.e., $\mathbf{g}^\pm(z, M_2)$, by using Eq. (4.5) again. To continue the partitioning process the region M_2 is divided into two regions, and so on. Thus it is straightforward to generalize the technique described in this subsection to the case of an arbitrary number of subslabs. This is done in the next two subsections.

4.2 Green operators for the subslabs

In the rest of this section the imbedded approach and the composite approach are presented for the general case of an arbitrary number of subslabs. In this subsection the general medium is described and the Green operators of the subslabs are introduced. The medium in question (denoted M_0) occupies the region $0 \le z \le L$ with vacuum in the regions $z < 0$ and $z > L$. The input on M_0 will be from the left only, but all results will carry over for the case of input from the right.

An imbedded slab of M_0 is any region $[\zeta_1, \zeta_2] = \{z : 0 \le \zeta_1 \le z \le \zeta_2 \le L\}$. Assume first that the medium is partitioned into $N + 1$ regions $[z_i, z_{i+1}]$, where $z_0 = 0$ and $z_{N+1} = L$, see Fig. 1. The imbedded slabs $[z_i, z_{i+1}]$ are denoted S_i and the imbedded slabs $[z_i, L]$ are denoted M_i. Defining the notation $S_i \cup S_{i+1}$ as a subslab defined in the region $[z_i, z_{i+2}]$ it follows that

$$M_i = \overset{N}{\underset{k=i}{\cup}} S_k \quad (i = 0, N), \qquad (4.9)$$

$$M_i = S_i \cup M_{i+1} \quad (i = 0, N-1). \qquad (4.10)$$

The Green operators of M_0 for input from the left are given in Eq. (3.1). The operators $\mathbf{g}^+$ and $\mathbf{g}^-$ of an imbedded slab $[z_i, z_j]$ are introduced accordingly as

$$\begin{pmatrix} \mathbf{g}^+(z, [z_i, z_j]) \\ \mathbf{g}^-(z, [z_i, z_j]) \end{pmatrix} E^+(z_i, t) = \begin{pmatrix} a(z_i, z) \\ 0 \end{pmatrix} E^+(z_i, t) +$$
$$+ \left[\begin{pmatrix} g^+(z, [z_i, z_j], \cdot) \\ g^-(z, [z_i, z_j], \cdot) \end{pmatrix} * E^+(z_i, \cdot) \right](t), \ z \in [z_i, z_j] \ (4.11)$$

and

$$\begin{pmatrix} \mathbf{f}^+(z, [z_i, z_j]) \\ \mathbf{f}^-(z, [z_i, z_j]) \end{pmatrix} E^-(z_j, t) = \begin{pmatrix} 0 \\ a(z, z_j) \end{pmatrix} E^-(z_j, t) + \qquad (4.12)$$
$$+ \left[\begin{pmatrix} f^+(z, [z_i, z_j], \cdot) \\ f^-(z, [z_i, z_j], \cdot) \end{pmatrix} * E^-(z_j, \cdot) \right](t), \ z \in [z_i, z_j],$$

where the arguments $(z, [z_i, z_j])$ indicate z as the point of evaluation and $[z_i, z_j]$ as the domain of the operators and kernels. The initial and boundary conditions of the kernels $g^\pm$ and $f^\pm$ are the same as for $G^\pm$ and $F^\pm$ in the previous section, i.e.,

$$\begin{cases} g^-(z, [z_i, z_j], 0) = -\frac{1}{4} a(z_i, z) \chi(z, 0) \\ f^+(z, [z_i, z_j], 0) = -\frac{1}{4} a(z, z_j) \chi(z, 0) \end{cases} \qquad (4.13)$$

$$\begin{cases} g^+(z_i, [z_i, z_j], t) = 0 \\ g^-(z_{i+1}, [z_i, z_j], t) = 0 \\ f^+(z_i, [z_i, z_j], t) = 0 \\ f^-(z_{i+1}, [z_i, z_j], t) = 0. \end{cases} \qquad (4.14)$$

If there is vacuum for $z > z_j$ then $(\mathbf{g}^+(z, [z_i, z_j]) + \mathbf{g}^-(z, [z_i, z_j])E^+(z_i, t)$ is the internal field at $z \in [z_i, z_j]$ from an incident field $E^+(z_i, t)$. If there is not vacuum for $z > z_j$ then that part of the medium will generate an incident field from the right, which will contribute to the internal field.

The relation in Eq. (4.5) also holds for the operators $\mathcal{G}^\pm(z)$ and $\mathbf{g}^\pm(z, M_i)$ and thus

$$\mathcal{G}^\pm(z) = \mathbf{g}^\pm(z, M_i)\mathcal{G}^+(z_i), \quad z \in M_i. \qquad (4.15)$$

Since the material parameters are assumed to be continuous across z_i, equation (4.15) can be written explicitly in terms of its kernels as

$$G^+(z, t) = a(z_i, z)G^+(z_i, t) + a(0, z_i)g^+(z, M_i, t) +$$
$$+ \left[g^+(z, M_i, \cdot) * G^+(z_i, \cdot) \right](t) \qquad (4.16)$$
$$G^-(z, t) = a(0, z_i)g^-(z, M_i, t) + \left[g^-(z, M_i, \cdot) * G^+(z_i, \cdot) \right](t), \ z \in M_i. \ (4.17)$$

Realizing that M_{i+1} is an imbedded part of M_i and also of M_0 the relation given in Eq. (4.15) can be generalized so that for $z \in M_{i+1}$, $\mathbf{g}^\pm(z, M_i)$ is expressed in terms of $\mathbf{g}^\pm(z, M_{i+1})$ via

$$\mathbf{g}^\pm(z, M_i) = \mathbf{g}^\pm(z, M_{i+1})\mathbf{g}^+(z_{i+1}, M_i), \quad z \in M_{i+1}. \qquad (4.18)$$

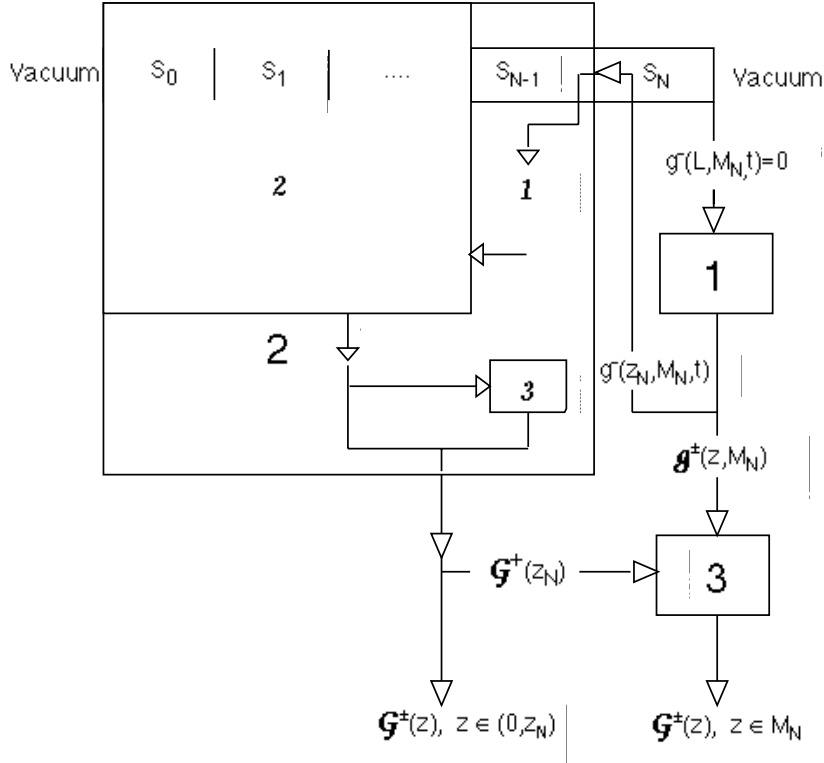Equation (4.18) is the underlying structure for the algorithms presented below.

Figure 2: A flowchart of the algorithm to generate $\mathcal{G}^{\pm}$, where the boxes 1, 2 and 3 correspond to the respective steps below.

4.3 The imbedded approach: An arbitrary number of sub-slabs

An algorithm based upon Eq. (4.15) with $i = N$ includes three steps. First $\mathbf{g}^{\pm}(z, M_N)$ is determined for $z \in M_N$. The kernel $g^-(z_N, M_N, t)$ is then used as a boundary condition when $\mathcal{G}^{\pm}(z)$ is determined for $z \in [0, z_N]$. Finally, $\mathcal{G}^+(z_N)$ is used to obtain $\mathcal{G}^{\pm}(z)$ for $z \in M_N$ using Eq. (4.15).

The region $[0, z_N]$ can now be broken into smaller pieces by using Eq. (4.18) recursively. A flowchart for the algorithm is given in Fig. 2, where the recursive part is indicated by the dotted lines.

In an iterative form the algorithm reads:

1. Start with the boundary condition $g^-(z_{N+1}, M_N, t) = 0$ and determine $g^{\pm}(z, M_N, t)$ for $z \in S_N$ from Eq. (3.9)

2. Do the following steps for $i = N - 1$ to $i = 0$

   Generate $g^{\pm}(z, M_i, t)$, $z \in S_i$, from Eq. (3.9) using

   $$g^-(z_{i+1}, M_i, t) =$$
   $$= a(z_i, z_{i+1}) g^-(z_{i+1}, M_{i+1}, t) + [g^-(z_{i+1}, M_{i+1}, \cdot) * g^+(z_{i+1}, M_i, \cdot)](t)$$

as the boundary condition at $z = z_{i+1}$ according to Eq. (4.18).

3. Since $g^\pm(z, M_0, t) = G^\pm(z, t)$, the Green operators for $z \in S_0$ are done at this stage. To obtain the Green operators for $z \in M_1$ the following steps are done for $i = 1$ to N according to Eq. (4.15)

$$
\begin{aligned}
G^+(z, t) =\ & a(z_i, z)G^+(z_i, t) + a(0, z_i)g^+(z, M_i, t) + \\
& + \left[g^+(z, M_i, \cdot) * G^+(z_i, \cdot)\right](t), \quad\quad\quad (4.19) \\
G^-(z, t) =\ & a(0, z_i)g^-(z, M_i, t) + \left[g^-(z, M_i, \cdot) * G^+(z_i, \cdot)\right](t), \ z \in S_i \ (4.20)
\end{aligned}
$$

4.4   The composite approach

The last subsection showed that one can find $G^\pm(z, t)$ from the Green operators of the imbedded slabs M_i. In this subsection, a modification is made to the algorithm so that one can find $\mathcal{G}^\pm(z)$ from $\mathbf{g}^\pm(z, S_i)$ and $\mathbf{f}^\pm(z, S_i)$. That is to find $\mathcal{G}^\pm(z)$ from the Green operators of subslabs S_i imbedded in vacuum. This method is appealing in the construction of the Green operators of composite media. The Green operators for each S_i can be generated and then stored. With such a data base, the Green operators for different composite media M_0 can be created by permuting the order of the subslabs. Also, calculating the Green operators for disjoint S_i gives a way to parallelize the numerical code. The derivation of the algorithm is based upon arguments used in the Redheffer star product, cf. [11] and [9].

It is possible to generate the Green operators $\mathbf{g}^\pm(z, M_i)$ from the operators of S_i and M_{i+1}, i.e., $\mathbf{g}^\pm(z, S_i)$, $\mathbf{f}^\pm(z, S_i)$ and $\mathbf{g}^\pm(z, M_{i+1})$. This is realized when one views $\mathbf{g}^-(z_{i+1}, M_{i+1})$ operating on $E^+(z_{i+1})$ as the input from the right on S_i. The input from the left and from the right on S_i are mapped to the internal fields by the operators $\mathbf{g}^\pm(z, S_i)$ and $\mathbf{f}^\pm(z, S_i)$. Thus for $z \in S_i$

$$
E^\pm\left(z, t + \frac{z - z_i}{c_0}\right) = \mathbf{g}^\pm(z, S_i)E^+(z_i, t) + \mathcal{L}^\pm(z, M_{i+1})E^+\left(z_i, t + \frac{z - z_i}{c_0}\right), \quad (4.21)
$$

where $\mathcal{L}^\pm(z, M_{i+1})E^+(z_i, t + \frac{z-z_i}{c_0})$ is that part of the field that is induced by M_{i+1}. Since from Eq. (3.1)

$$
E^\pm\left(z, t + \frac{z - z_i}{c_0}\right) = \mathbf{g}^\pm(z, M_i)E^+(z_i, t) \quad\quad\quad (4.22)
$$

the following fundamental relation is obtained

$$
\mathbf{g}^\pm(z, M_i)E^+(z_i, t) = \mathbf{g}^\pm(z, S_i)E^+(z_i, t) + \mathcal{L}^\pm(z, M_{i+1})E^+\left(z_i, t + \frac{z - z_i}{c_0}\right), \ z \in S_i. \quad (4.23)
$$

The operator $\mathcal{L}$ can be expressed in terms of the Green operators. To do this it is first observed from Eq. (4.12) that

$$
\mathcal{L}^\pm(z, M_{i+1})E^+(z_i, t) = \mathbf{f}^\pm(z, S_i)E^-\left(z_{i+1}, t + \frac{z - z_{i+1}}{c_0}\right) \quad\quad (4.24)
$$

where $E^-(z_{i+1}, t)$ is related to $E^+(z_i, t)$ by

$$
\begin{aligned}
E^-(z_{i+1}, t) &= \mathbf{g}^-(z_{i+1}, M_{i+1}) \left(\mathbf{g}^+(z_{i+1}, S_i) E^+(z_i, t - (z_{i+1} - z_i)/c_0) + \right. \\
&\quad \left. + \mathbf{f}^+(z_{i+1}, S_i) E^-(z_{i+1}, t) \right).
\end{aligned}
\tag{4.25}
$$

By a formal operation the field $E^-(z_{i+1}, t)$ can be eliminated and since $E^+(z_i, t)$ is an arbitrary incident field the expression for $\mathcal{L}$ is obtained

$$
\begin{aligned}
\mathcal{L}^\pm(z, M_{i+1}) &= \\
&= \mathbf{f}^\pm(z, S_i) \left[1 - \mathbf{g}^-(z_{i+1}, M_{i+1}) \mathbf{f}^+(z_{i+1}, S_i) \right]^{-1} \mathbf{g}^-(z_{i+1}, M_{i+1}) \mathbf{g}^+(z_{i+1}, S_i).
\end{aligned}
\tag{4.26}
$$

From the expressions in Eqs. (4.21)-(4.26) it is seen that the contribution

$$
\mathcal{L}^\pm(z, M_{i+1}) E^+(z_i, t + \frac{z - z_i}{c_0})
\tag{4.27}
$$

in Eq. (4.21) reaches the point z a time $2(z_{i+1} - z)/c_0$ later than the contribution $\mathbf{g}^\pm(z, S_i) E^+(z_i, t)$, as expected. The time delay $(z - z_i)/c_0$ in the second term of the right hand side of Eq. (4.21) was introduced to avoid explicit time delays in the operator expression in Eq. (4.26).

The inverse operator appearing in Eq. (4.26) can be expressed in terms of a resolvent kernel $K_{i+1}(t)$ as

$$
\left[1 - \mathbf{g}^-(z_{i+1}, M_{i+1}) \mathbf{f}^+(z_{i+1}, S_i) \right]^{-1} E(t) = E(t) + \left[K_{i+1}(\cdot) * E(\cdot) \right](t)
\tag{4.28}
$$

from which it is seen that the kernel $K_{i+1}(t)$ satisfies the Volterra equation of the second kind

$$
\begin{aligned}
K_{i+1}(t) &- \left[g^-(z_{i+1}, M_{i+1}, \cdot) * f^+(z_{i+1}, S_i, \cdot) \right](t) - \\
&- \left[g^-(z_{i+1}, M_{i+1}, \cdot) * f^+(z_{i+1}, S_i, \cdot) * K_{i+1}(\cdot) \right](t) = 0.
\end{aligned}
\tag{4.29}
$$

The kernel $K_{i+1}(t)$ also may be obtained by expanding the inverse operator in Eq. (4.26) in a power series

$$
\begin{aligned}
\left[1 - \mathbf{g}^-(z_{i+1}, M_{i+1}) \mathbf{f}^+(z_{i+1}, S_i) \right]^{-1} E(t) &= \\
= E(t) + \sum_{n=1}^{\infty} (\mathbf{g}^-(z_{i+1}, M_{i+1}) \mathbf{f}^+(z_{i+1}, S_i))^n E(t) &= \\
= E(t) + \left[\sum_{n=1}^{\infty} (g^-(z_{i+1}, M_{i+1}, \cdot) * f^+(z_{i+1}, S_i, \cdot) *)^n E \right](t)
\end{aligned}
\tag{4.30}
$$

thus

$$
K_i(t) = \left[\sum_{n=1}^{\infty} (g^-(z_i, M_i, \cdot) * f^+(z_i, S_{i-1}, \cdot) *)^{n-1} g^-(z_i, M_i, \cdot) * f^+(z_i, S_{i-1}, \cdot) \right](t).
\tag{4.31}
$$

From a general convergence proof for functional power series given in [13] it is seen that the series in Eq. (4.31) converges for all times if the kernels $g^-(z_{i+1}, M_{i+1}, t)$ and $f^+(z_{i+1}, S_i, t)$ are bounded. The rate of convergence depends on the behavior of the kernels $g^-(z_{i+1}, M_{i+1}, t)$ and $f^+(z_{i+1}, S_i, t)$ and might be hard to analyze a priori.

The relations in Eq. (4.26) are a generalization of the Redheffer star product [11] used to find the reflection and transmission operators of M_i, from the respective operators of S_i and M_{i+1}.

The numerical implementation of these ideas involves the following three steps:

1. First generate $g^\pm(z, S_i)$ and $f^\pm(z, S_i)$, $z \in S_i$ for $i = 0$ to $i = N$ by numerically solving Eqs. (3.9) and (3.12). Notice that $g^\pm(z, M_N, t) = g^\pm(z, S_N, t)$ for $z \in S_N$.

2. Use the "gluing" procedure described by Eq. (4.26) i.e., do the following steps for $i = N$ to $i = 1$

   Solve Eq. (4.29) for $K_i(t)$ or use the series in Eq. (4.31) to obtain $K_i(t)$

   Introduce the kernel $I_i^-(t)$ as

   $$I_i^-(t) = a(z_{i-1}, z_i) \left(g^-(z_i, M_i, t) + [K_i(\cdot) * g^-(z_i, M_i, \cdot)](t) \right) +$$
   $$+ [g^-(z_i, M_i, \cdot) * g^+(z_i, S_{i-1}, \cdot)](t) +$$
   $$[g^-(z_i, M_i, \cdot) * g^+(z_i, S_{i-1}, \cdot) * K_i(\cdot)](t)$$

   Generate $g^\pm(z, M_{i-1}, t)$ for $z \in S_{i-1}$ via

   $$g^+(z, M_{i-1}, t) = g^+(z, S_{i-1}, t) + \left[f^+(z, S_{i-1}, \cdot) * I_i^-(\cdot) \right](t - 2(z_i - z)/c_0)$$
   $$g^-(z, M_{i-1}, t) = g^-(z, S_{i-1}, t) + a(z, z_i) I_i^-(t - 2(z_i - z)/c_0) +$$
   $$+ \left[f^-(z, S_{i-1}, \cdot) * I_i^-(\cdot) \right](t - 2(z_i - z)/c_0)$$

3. Update $\mathcal{G}^\pm$ for the region $z \in M_1$ by doing step 3 in the algorithm in the subsection above, i.e., for $i = 1$ to N

$$
\begin{aligned}
G^+(z, t) =\ & a(z_i, z) G^+(z_i, t) + a(0, z_i) g^+(z, M_i, t) + \\
& + \left[g^+(z, M_i, \cdot) * G^+(z_i, \cdot) \right](t), & (4.32) \\
G^-(z, t) =\ & a(0, z_i) g^-(z, M_i, t) + \left[g^-(z, M_i, \cdot) * G^+(z_i, \cdot) \right](t), \ z \in S_i & (4.33)
\end{aligned}
$$

This method assumes that the impedance is continuous across the interfaces. That is always the case when the media are dispersive and described by the constitutive relation in Eq. (2.2). The continuity is manifest in that $g^-(z, M_i, t) = g^-(z, (z_i, L], t)$ where $(z_i, L]$ then denotes the region $z_i < z \le L$. These kernels are not equal to each other if two dissimilar materials are interfaced at $z = z_i$ such that there will be an impedance mismatch at that point. To see how this comes about assume that two stratified media of arbitrary composition are interfaced together. Assume the following general boundary conditions for the Maxwell equations characterized by an operator valued matrix $\mathbf{B}$

$$\begin{pmatrix} E \\ \partial_z E \end{pmatrix} (z_i^-, t) = \mathbf{B} \begin{pmatrix} E \\ \partial_z E \end{pmatrix} (z_i^+, t). \tag{4.34}$$

Applying the respective splitting of each medium to the above equation (they might not be a vacuum splitting) one has as the interfacing operator

$$\begin{pmatrix} E^+ \\ E^- \end{pmatrix} (z_i^-, t) = \mathbf{P}(z_i^-)\mathbf{B}\mathbf{P}^{-1}(z_i^+) \begin{pmatrix} E^+ \\ E^- \end{pmatrix} (z_i^+, t) = \mathbf{T} \begin{pmatrix} E^+ \\ E^- \end{pmatrix} (z_i^+, t). \quad (4.35)$$

The reflection properties of the interface will now be extracted from Eq. (4.35). Noting that $E^-(z_i^+, t) = \mathbf{g}^-(z_i^+, (z_i, L])E^+(z_i^+, t)$ and using Eq. (4.35) the following relation is formed

$$E^-(z_i^-, t) = \left[T_{21} + T_{22}\mathbf{g}^-(z_i^+, (z_i, L]) \right] \left[T_{11} + T_{12}\mathbf{g}^-(z_i^+, (z_i, L]) \right]^{-1} E^+(z_i^-, t), \quad (4.36)$$

Since $E^-(z_i^-, t) = \mathbf{g}^-(z_i^-, [z_i, L])E^+(z_i^-, t)$ it follows that

$$\mathbf{g}^-(z_i^-, [z_i, L]) = \left[T_{21} + T_{22}\mathbf{g}^-(z_i^+, (z_i, L]) \right] \left[T_{11} + T_{12}\mathbf{g}^-(z_i^+, (z_i, L]) \right]^{-1}. \quad (4.37)$$

It is assumed that the inverse of the operator expression in the above equation does exist. The actual validity of that statement will be taken on a case by case basis.

As an example consider an interface that has a dielectric medium on the left and a dispersive medium on the right. The wave equation for the dielectric medium is

$$\partial_z \begin{pmatrix} E \\ \partial_z E \end{pmatrix} (z, t) = \begin{pmatrix} 0 & 1 \\ \frac{1}{c(z)^2}\partial_t^2 & 0 \end{pmatrix} \begin{pmatrix} E \\ \partial_z E \end{pmatrix} (z, t) \quad (4.38)$$

and is put into normal form via the splitting

$$\mathbf{P}(z) = \begin{pmatrix} 1 & -c(z)\partial_t^{-1} \\ 1 & c(z)\partial_t^{-1} \end{pmatrix}. \quad (4.39)$$

From the boundary conditions of the Maxwell equations it is shown that

$$\begin{pmatrix} E \\ \partial_z E \end{pmatrix} (z_i^-, t) = \begin{pmatrix} E \\ \partial_z E \end{pmatrix} (z_i^+, t), \quad \text{i.e. } \mathbf{B} = \mathbf{I}, \quad (4.40)$$

and by applying the splittings for the respective media one obtains

$$\begin{pmatrix} E^+ \\ E^- \end{pmatrix} (z_i^-, t) = \frac{1}{2} \begin{pmatrix} 1 + \frac{c(z_i^-)}{c_0} & 1 - \frac{c(z_i^-)}{c_0} \\ 1 - \frac{c(z_i^-)}{c_0} & 1 + \frac{c(z_i^-)}{c_0} \end{pmatrix} \begin{pmatrix} E^+ \\ E^- \end{pmatrix} (z_i^+, t). \quad (4.41)$$

Using Eq. (4.37) as motivation one obtains

$$E^-(z_i^-, t) = \left[\left[r + g^-(z_i^+, (z_i, L], \cdot)* \right] \left[1 + rg^-(z_i^+, (z_i, L], \cdot)* \right]^{-1} E^+(z_i^-, \cdot) \right] (t), \quad (4.42)$$

where the reflection coefficient is given by

$$r = \frac{c_0 - c(z_i^-)}{c_0 + c(z_i^-)}. \quad (4.43)$$

The inverse operator that appears in Eq. (4.42) may be expressed in terms of the resolvent kernel $J(t)$ as

$$\left[\left[1 + rg^-(z_i^+, (z_i, L], \cdot)*\right]^{-1} E^+(z_i^-, \cdot)\right](t) = E^+(z_i^-, t) + \left[J(\cdot) * E^+(z_i^-, \cdot)\right](t).$$
(4.44)

The kernel $J(t)$ then satisfies the resolvent equation

$$rg^-(z_i^+, (z_i, L], t) + J(t) + r\left[g^-(z_i^+, (z_i, L], \cdot) * J(\cdot)\right](t) = 0.$$
(4.45)

5   Numerical examples

In this section the generalized Green functions technique described in section (3) and (4) is applied to an inhomogeneous dispersive medium. In section 4 two different ways to relate the Green operators of a dispersive medium to the Green operators of the subslabs of the medium were described. One was based upon the imbedding technique and the other on the Redheffer star product. In the examples presented in this section only the technique based upon the imbedding technique has been used. The other technique is expected to give identical results.

The two most commonly used models for dispersion in electromagnetics are the Debye model and the Lorentz model, cf eg. [14] and [15]. First these two models will be discussed and for this purpose the following notations are introduced:

$$
\begin{aligned}
q &= \text{electron charge} \\
m &= \text{electron mass} \\
N &= \text{electron density} \\
\omega_0 &= \text{the harmonic frequency for an electron bound to an atom} \\
\nu &= \text{the collision frequency for an electron} \\
\tau &= \text{the relaxation time for the molecular polarization} \\
\omega_p &= \sqrt{\frac{Nq^2}{\varepsilon_0 m}} = \text{the plasma frequency.}
\end{aligned}
$$

The resonance or the Lorentz model is appropriate for most solid materials. The basic assumption in this model is that the electron is affected by a restoring harmonic force and a friction force proportional to the velocity of the electron. The explicit expression for the susceptibility kernel then follows from the equation of motion for the electron

$$\chi(\boldsymbol{r}, t) = \omega_p^2(\boldsymbol{r}) \frac{\sin \nu_0(\boldsymbol{r}) t}{\nu_0(\boldsymbol{r})} e^{-\nu(\boldsymbol{r}) t/2}$$
(5.1)

where $\nu_0^2(\boldsymbol{r}) = \omega_0^2(\boldsymbol{r}) - \nu^2(\boldsymbol{r})/4$.

The second type of susceptibility kernel is appropriate for liquids. The basic assumption in this model is that the polarization of the medium is caused by the permanent polarization of the molecules. These molecules align to an electric field $\boldsymbol{E}(\boldsymbol{r}, t)$ with a rate $\alpha(\boldsymbol{r})$ and the relaxation of the polarization is modeled by the

relaxation time $\tau(\boldsymbol{r})$. From this assumption the relaxation model or Debye model follows

$$\chi(\boldsymbol{r}, t) = \alpha(\boldsymbol{r}) e^{-t/\tau(\boldsymbol{r})}. \tag{5.2}$$

Normally the susceptibility kernel for a medium is the sum of several Lorentz or Debye kernels, cf Ref. [14].

If the variation in time of the electric field is slow compared to the variation of the susceptibility kernel, the approximate constitutive relation $\boldsymbol{D}(\boldsymbol{r}, t) = \varepsilon_0 \varepsilon_r(\boldsymbol{r}) \boldsymbol{E}(\boldsymbol{r}, t)$. can be used. From Eqs. (5.1) and (5.2) it follows that in a first order approximation

$$\varepsilon_r(\boldsymbol{r}) = 1 + (\omega_p(\boldsymbol{r})/\omega_0(\boldsymbol{r}))^2 \tag{5.3}$$
$$\varepsilon_r(\boldsymbol{r}) = 1 + \alpha(\boldsymbol{r})\tau(\boldsymbol{r}) \tag{5.4}$$

for the Lorentz and Debye model, respectively. Thus if ω_0 is a high frequency in a Lorentz medium and if τ is a short time in a Debye medium then propagation of transient waves in these media is expected to resemble that in non-dispersive dielectric media. That this is the case will be shown by some numerical results in this section.

In the examples all media considered are of length $L = 1\,\mathrm{m}$. Outside the medium there is vacuum. Wave propagation in the following media will be considered:

medium 1: dielectric; $\varepsilon_r = 1 + 1.25\sin(\pi z)$

medium 2: Debye; $\tau = 6 \times 10^{-11}\,s$, $\alpha = \dfrac{1.25}{\tau}\sin(\pi z)\,s^{-1}$

medium 3: Debye; $\tau = 2 \times 10^{-10}\,s$, $\alpha = \dfrac{1.25}{\tau}\sin(\pi z)\,s^{-1}$

medium 4: Lorentz; $\nu = 0\,s^{-1}$, $\omega_p = \sqrt{1.25\sin(\pi z)}\,10^{-10}\,s^{-1}$, $\omega_0 = 10^{10}\,s^{-1}$

The permittivity profile is seen in Fig. 3. The values of the parameters in the three dispersive media are chosen so that the permittivities in Eqs. (5.3) and (5.4) are identical with the permittivity for the dielectric medium. It will be seen that the two Debye media respond almost as the dielectric medium even for an incident delta pulse. The Lorentz medium is seen to be completely different from the dielectric medium for an incident delta pulse, whereas they respond almost identical to an incident ramp.

In the graphs the fields and times are normalized with the speed of light in vacuum. Thus one unit of the normalized time equals the travel time through one meter of vacuum. Two roundtrips of data have been calculated, as seen from the figures. For the dispersive media the same discretization has been used in all examples. The media were divided in 32 slabs, where every slab was discretized in 32 steps in z and 2048 steps in time using a constant stepsize. The equations for the Green kernels, Eq. (3.9), as well as the convolutions in Eq. (2.1) were calculated by the trapezoidal rule. The original Green functions method using the trapezoidal rule for the discretization of the equations would need a grid with 1024 by 2048
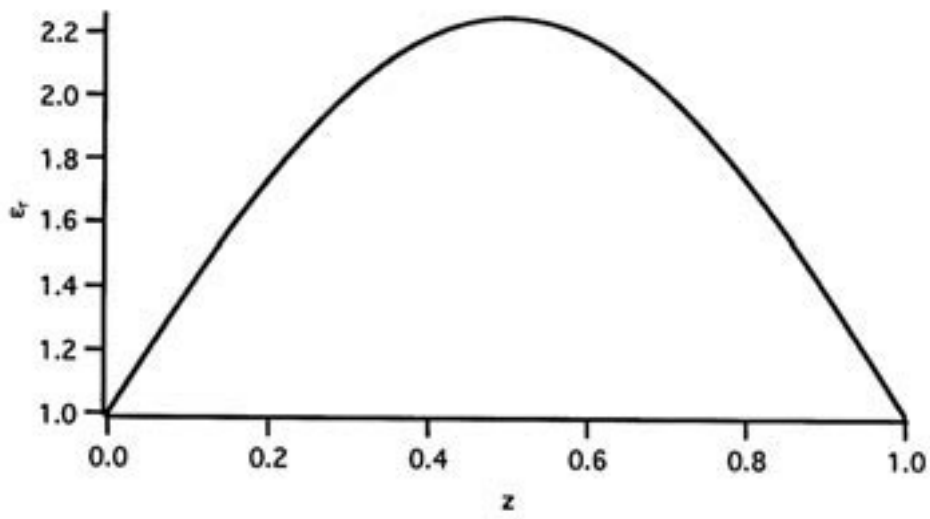
Figure 3: The permittivity profile, $\varepsilon_r = 1+1.25\sin(\pi z)$, used for the non-dispersive media in Figs. 4-12.
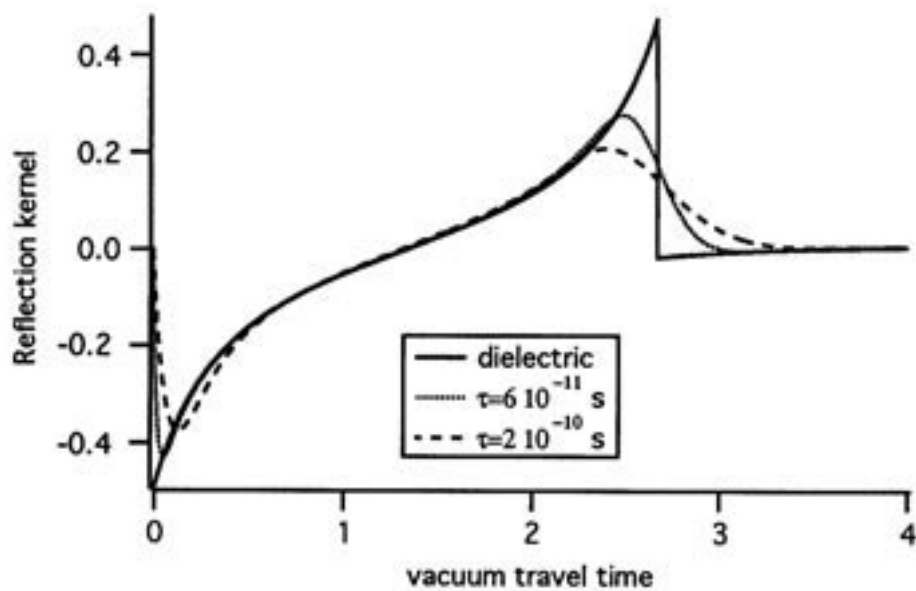

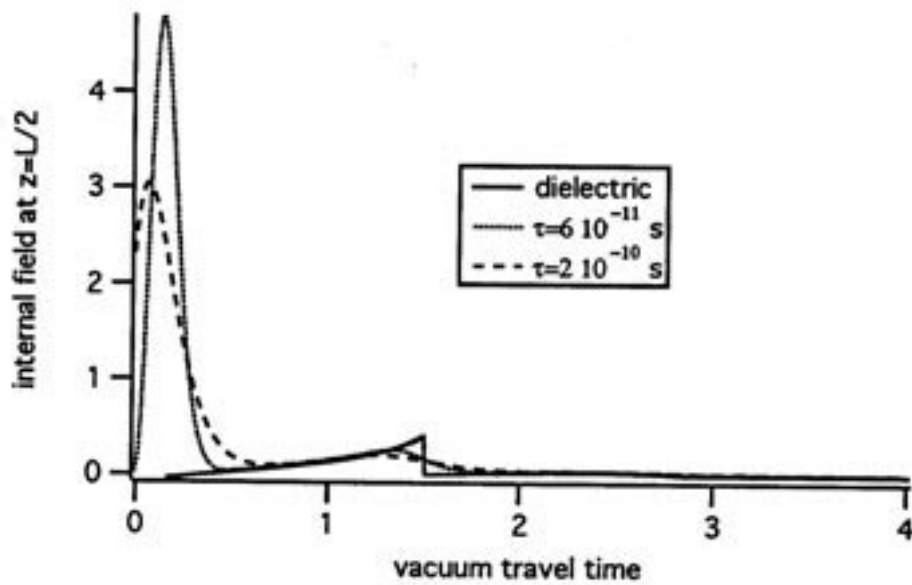**Figure 4**: Reflected fields due to an incident delta pulse (Debye and dielectric) for the media 1,2 and 3.

Figure 5: Internal fields in the middle of the slab due to an incident delta pulse for the media 1, 2 and 3.
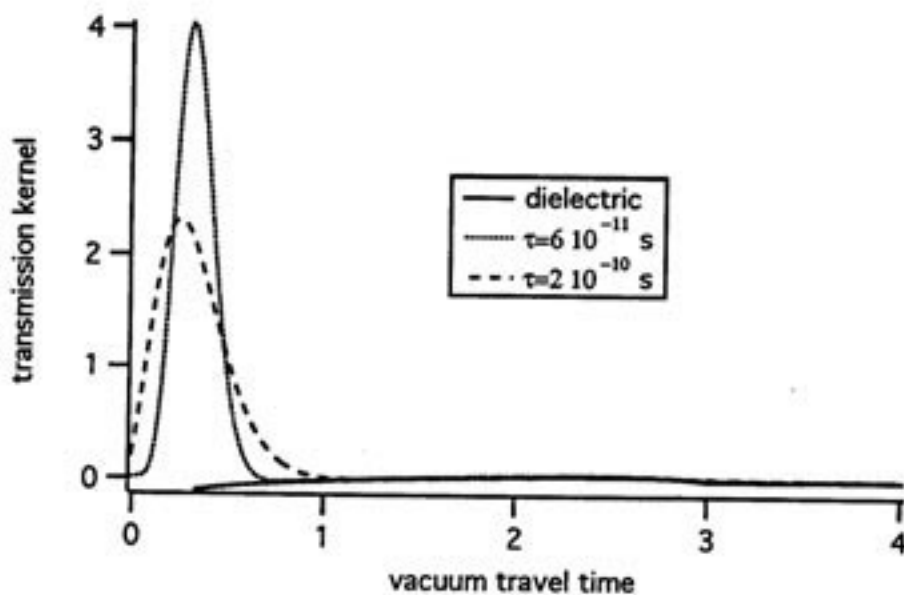

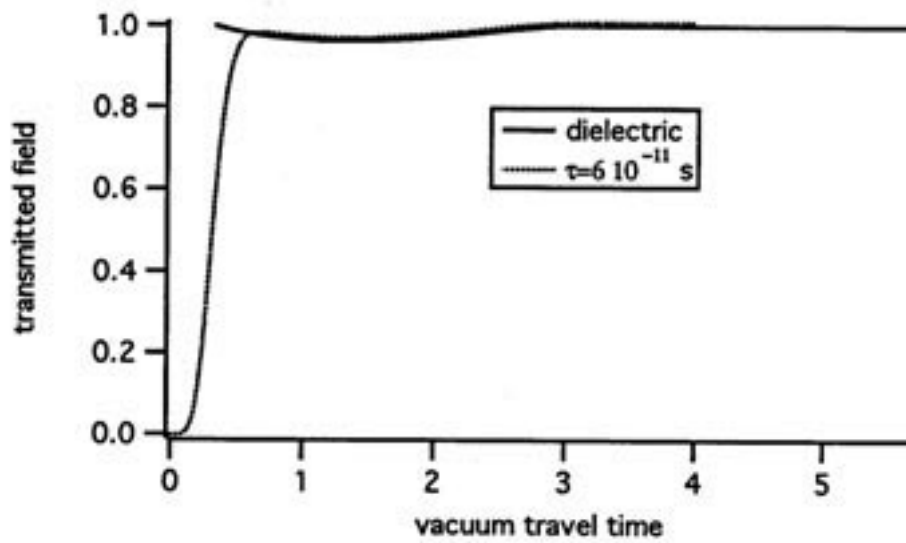**Figure 6**: Transmitted fields due to an incident delta pulse for the media 1, 2 and 3.

Figure 7: Transmitted fields due to an incident step function for the media 1, 2 and 3. The curves are the time integrals of the corresponding curves in Fig. 6.
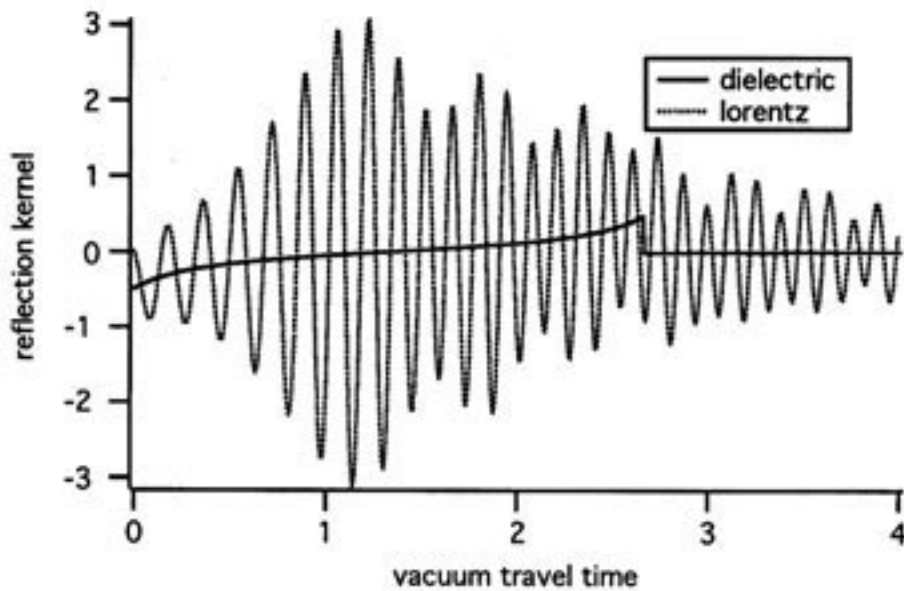

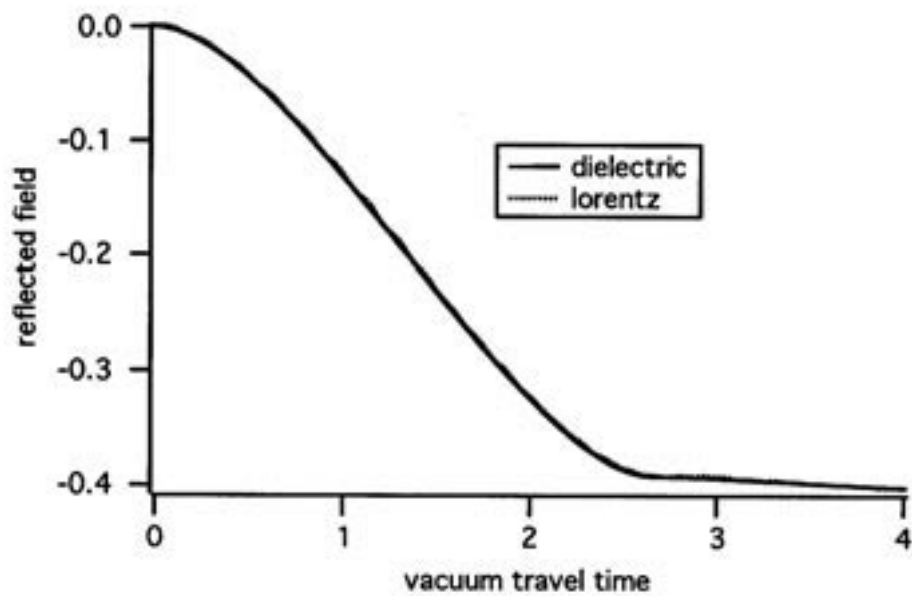**Figure 8**: Reflected fields due to an incident delta pulse for the media 1 and 4.

Figure 9: Reflected fields due to an incident ramp for the media 1 and 4. The curves are obtained by integrating the curves in Fig. 8 twice.
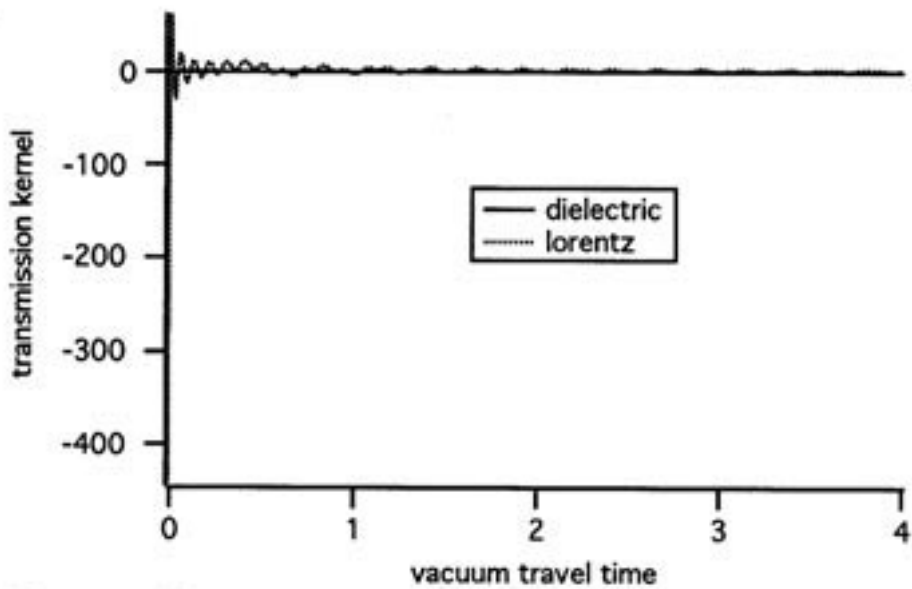

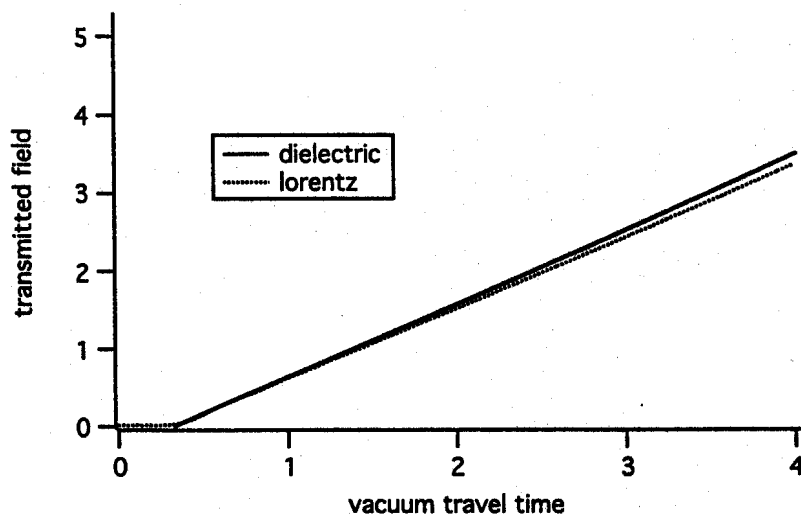**Figure 10**: Transmitted fields due to an incident delta pulse for media 1 and 4.

Figure 11: Transmitted fields due to an incident ramp for media 1 and 4.The curves are the time integrals of the corresponding curves in Fig. 10.
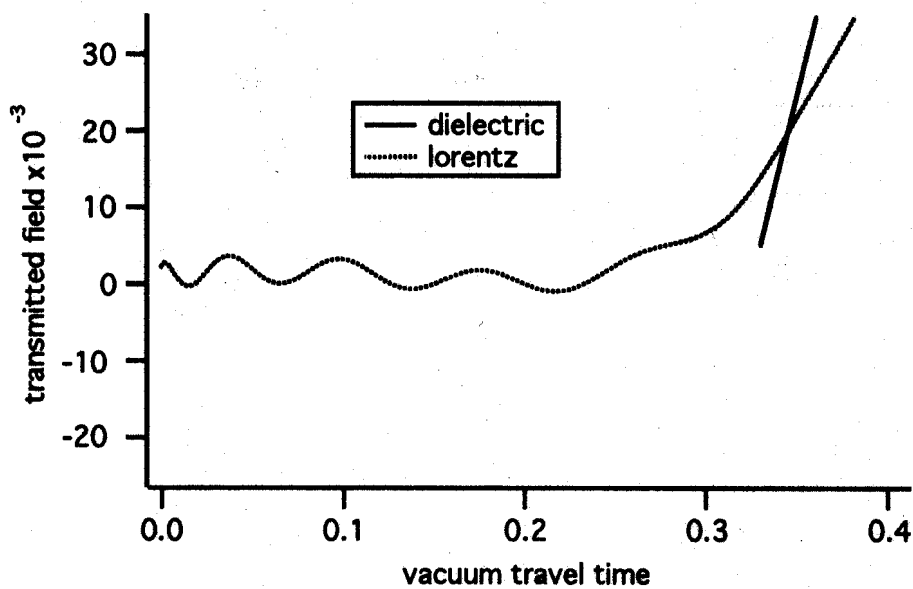

Figure 12: The early time behavior of the transmitted field due to an incident ramp for the Lorentz medium, medium 4, and the dielectric medium, medium 1. The curves are a blowup of the early part of the curves in Fig. 11. The curve for the Lorentz medium is the Sommerfeld precursor.

points. That would require an internal memory of about 20 Mbyte, whereas the new technique only requires approximately 2 Mbyte.

It should be pointed out that using the Green functions method for Debye or Lorentz media one can use a trick to save memory and increase speed. The trick is to write the convolution integrals in Eq. (3.9) as

$$\chi_d * G = e^{-t/\tau} \int_0^t e^{t'/\tau} G(t') dt'$$

$$\chi_l * G = \frac{e^{-\nu t/2}}{\nu} \left(\sin(\nu_0 t) \int_0^t e^{\nu t'/2} \cos(\nu_0 t') dt' - \cos(\nu_0 t) \int_0^t e^{\nu t'/2} \sin(\nu_0 t') dt' \right).$$

By using these expressions, the Green kernels do not have to be saved at all grid-points. It is enough to save them at the last time step for all $z-$ points. Also the convolution from the previous timestep is then used to get the convolution at the next time step and that increases the speed considerably. However, these tricks have not been used in the numerical examples.

In the first example, Fig. 4, the reflection kernels for media 1, 2 and 3 are presented. The reflection kernels correspond to the reflected field generated by an incident delta pulse. It is interesting to see that even here the reflected fields for the Debye media are close to the one for the dielectric. The discontinuity in the reflection kernel for the dielectric is due to the discontinuity of the derivative of the wave velocity at $z = L$, cf [1]. The delta pulse response, i.e., $G^+ + G^-$, at $z = 0.5\,m$ and $z = 1\,m$ is given in Figs. (5) and (6), respectively. It should be noticed that the total wave for the dielectric medium has a delta pulse contribution at the wave front that of course is not shown in Figs. (5) and (6). The transmitted fields from an incident step function of unit height are given in Fig. 7. These fields are simply the integral of the fields in Fig. 6 except that the integrals over the delta function contributions were added.

The comparison between the Lorentz medium and the dielectric medium is shown in Figs. (8)-(12). Figure (8) gives the reflection kernels for the two media. These kernels do not resemble each other too well. If the kernels are integrated twice the resulting fields are the responses for an incident ramp, i.e., $E^i(0, t) = t$, and then the fields are almost identical, as seen in Fig. 9. In Figs. 10 and 11 the transmitted fields from an incident delta pulse and ramp, respectively are shown. The difference in the delta pulse responses is then significant and yet the same fields integrated twice are almost identical. The difference that can be seen in Fig. 11 is due to numerical errors and could have been eliminated by reducing the step size by a factor of two. The last example, Fig. 12, is a blowup of the part of the transmitted field in Fig. 11 that arrived before the main signal arrives. This is the precursor. As expected it has the same behavior as the Sommerfeld precursor for a homogeneous medium, cf [15]. It would be very interseting if also the second (Brillouin) precursor could be seen. The authors have tried to obtain also this precursor by the present technique. To clearly see the second precursor it should be separeted from the first precursor in time. This is the case if the medium is long enough. However when the medium is made longer the first precursor oscillates more rapidly and thus a smaller gridsize has to be used in both time and space. Quite soon the limit of the capacity of the

computer is reached, even using the partitioning techniques discussed in this paper. So far the authors have not been able to produce a case where the second precursor is clearly seen. An extensive survey of precursors and wave propagation in dispersive media using frequency domain methods is found in [16].

Conclusions

The technique developed in this paper may be viewed as a tool for problems concerning transient wave propagation in linear media. From the technique, algorithms for wave propagation problems can be obtained that are fast and do not require large internal memories. An advantage is that these algorithms can be implemented on computers using parallel processors. An important class of problems to which the technique in this paper is directly applicable is wave propagation in composite media. The media can then be composed of slabs of different types of materials, such as isotropic, anisotropic and chiral materials. A subclass of composite media is periodic media. For periodic media the partitioning technique in this paper uses the periodicity of the media in a smart way to solve the wave propagation problems in these media. A project concerning this application is currently under development.

References

[1] Krueger R. J. and Ochs R. L., "A Green's Function Approach to the Determination of internal Fields," *Wave Motion*, **11**, 525-543 (1989).

[2] Kristensson G., Karlsson A. and Otterheim H., "Transient wave propagation in gyrotropic media," *proceeddings of the 858th AMS meeting 1990*

[3] Karlsson A., Otterheim H and Stewart R., "Electromagnetic fields in an inhomogeneous plasma from obliquely incident transient plane waves," Technical report TRITA-TET 91-2, Royal Institute of Technology, Stockholm, Sweden, June 1991

[4] Kristensson. G., "Direct and inverse scattering problems in dispersive media– Green's functions and invariant imbedding techniques," In Kleinman R., Kress R., and Martensen E.,editors, *Direct and Inverse Boundary Value problems*, Methoden und Verfahren der Mathematischen Physik, Band 37, pp 105–119, Mathematisches Forschungsinstitut Oberwolfach, FRG,1989.

[5] Corones J. P., Davison M. E. and Krueger R. J., "Direct and inverse scattering in the time domain via invariant imbedding equations," *J. Acoust. Soc. Am.*, **74**, 1535–1541, 1983.

[6] Ammicht E., Corones J. P. and Krueger R. J., "Direct and inverse scattering for viscoelastic media," *J. Acoust. Soc. Am.*, **81**, 827–834, 1987.

[7] Kristensson G. and Krueger R. J., "Direct and inverse scattering in the time domain for a dissipative wave equation. Part I. Scattering operators," *J. Math. Phys.*, **27**,1667-82, 1986.

[8] Kristensson G. and Krueger R. J., "Direct and inverse scattering in the time domain for a dissipative wave equation. Part II. Simultaneous reconstruction of dissipation and phase velocity profiles," *J. Math. Phys.*, **27**, 1683-93, 1986.

[9] Kristensson G. and Krueger R. J., "Direct and inverse scattering in the time domain for a dissipative wave equation. Part III. Scattering operators in the presence of a phase velocity mismatch," *J. Math. Phys.*, **28**,360-370, 1987.

[10] Bruckstein A. M., Levy B. C. and Kailath T, "Differential methods in inverse scattering," *SIAM J. Appl. Math.*, **45**, 312–335, 1985.

[11] Redheffer R., "On the relation of transmission-line theory to scattering and transfer," *J. Math. and Phys.*, **41**, 1-41, 1962.

[12] Karlsson A. and Kristensson G., "Constitutive relations, dissipation and reciprocity for the Maxwell equations in the time domain," *J. of EM waves and appl.* (to appear)

[13] Volterra V., *Theory of Functionals,* Blackie & Son Limited, London (1930), p. 102

[14] Bohren C. F. and Huffman D. R., *Absorption and Scattering of Light by Small Particles*, (Wiley, New York, 1983).

[15] Jackson J.D., *Classical Electrodynamics*, (Wiley, New York 1975).

[16] Oughstun K. E. and Sherman G. C., "Propagation of Electromagnetic Pulses in a Linear Dispersive Medium with Absorption (the Lorentz medium)," *J. Opt. Soc. Am. B*, **5**(4), 817-849 (1988).